DETAILED STUDY OF THE QUARK–ANTIQUARK FLUX TUBES AND FLUX TUBE RECOMBINATION*

Marco Cardoso, Pedro Bicudo, Nuno Cardoso

CFTP, Instituto Superior Técnico, Universidade Técnica de Lisboa
Avenida Rovisco Pais,1, 1049-001 Lisboa, Portugal

In this work, we compute the color fields in the mediator plane between a static quark and a static antiquark using quenched lattice QCD. In particular, we see the effect of the quark–antiquark distance on the flux tube. To obtain this results, an improved multihit technique is developed and an extend smearing technique is used. Then, we also discuss the flux-tubes in a system composed of two quarks and two antiquarks. The ground and first excited states fields are studied for different dispositions of the system.

1. Introduction

This work is divided in two parts. In the first one, we will study an isolated fundamental flux-tube in a quark–antiquark system. In the second one, we will study the fields in a system made of two quarks and two antiquarks, where we can observe the interaction between two fundamental flux tubes.

2. Chromo-fields computation

To calculate the gauge invariant squared chromoelectric and chromomagnetic fields in the lattice, we only have to calculate the correlation of the Wilson loop operator W which in large Euclidean time limit $t \to \infty$ should describe the static system, with the plaquettes corresponding to each of the fields. Concretely, we have

$$\left\langle E_i^2 \right\rangle = \left\langle P_{0i} \right\rangle - \frac{\langle W\, P_{0i} \rangle}{\langle W \rangle}, \tag{1}$$

$$\left\langle B_i^2 \right\rangle = \frac{\langle W\, P_{jk} \rangle}{\langle W \rangle} - \left\langle P_{jk} \right\rangle, \tag{2}$$

---

where $P_{\mu\nu} = 1 - \frac{1}{3}\text{Tr}[U_\mu(\boldsymbol{s})U_\nu(\boldsymbol{s}+\boldsymbol{\mu})U_\mu^\dagger(\boldsymbol{s}+\boldsymbol{\nu})U_\nu^\dagger(\boldsymbol{s})]$. The spatial indices j and k complement index i. The Lagrangian density is given by $\mathcal{L} = \frac{1}{2}(E^2 - B^2)$.

3. Fundamental flux-tube

For a simple quark–antiquark singlet, the Wilson Loop operator W describes the system. We compute the chromo-fields in the mediator plane between the quark and the antiquark, using 1100 pure gauge 32^4 configurations with $\beta = 6.0$. In order to improve the signal to noise ratio, we use two techniques: an improved version of the multihit [1] and an extended spatial smearing technique.

3.1. Signal to noise ratio improvement

In the multihit method, we replace each temporal link by its thermal average, with its first neighbors fixed, that is $U_4 \to \overline{U}_4 = \frac{\int dU_4\, U_4\, e^{\beta \text{Tr}[U_4 F^\dagger]}}{\int dU_4\, e^{\beta \text{Tr}[U_4 F^\dagger]}}$.

We generalize this method by replacing each temporal link by its thermal average with the Nth neighbors fixed, that is

$$U_4 \to \overline{U}_4 = \frac{\int [\mathcal{D}U]_\Omega\, U_4\, e^{\beta \sum_{\mu \boldsymbol{s}} \text{Tr}\left[U_\mu(\boldsymbol{s})F_\mu^\dagger(\boldsymbol{s})\right]}}{\int [\mathcal{D}U]_\Omega\, e^{\beta \sum_{\mu \boldsymbol{s}} \text{Tr}\left[U_\mu(\boldsymbol{s})F_\mu^\dagger\right]}}. \tag{3}$$

In this way, we have an error reduction greater than the one of multihit.

To increase the ground state overlap, we use a spatial extended smearing

$$U_i \to \mathcal{P}_{\text{SU}(3)}\left[U_i + w_1 \sum_j S_{ij}^1 + w_2 \sum_j S_{ij}^2 + w_3 \sum_j S_{ij}^3\right] \tag{4}$$

with staples S_{ij}^1, S_{ij}^2 and S_{ij}^3 being given in Fig. 1.

Even using this technique we were not able to find a value of t for which the plaquettes to Wilson Loop correlators are stable within error bars, while still have a sufficiently high signal-to-noise ratio. To solve this, we note that the correlator which gives the average of field $\langle F \rangle$ should be given by the formula $\langle F \rangle_t = \langle F \rangle_\infty + b\, e^{-\Delta t}$ for large values of t, with $\Delta = V_1 - V_0$, being the difference between the first excited and the ground state potentials. To compute Δ, we use a variational basis of four levels of APE smearing, with the potentials V_1 and V_0 being given by the solution of the variational generalized eigensystem

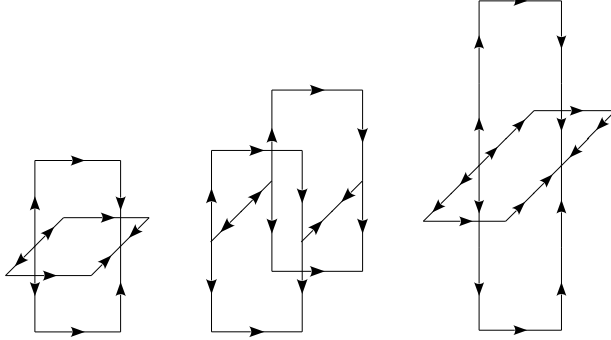$$\langle W_{ij}(t)\rangle c_j^n(t) = w_n(t)\langle W_{ij}(0)\rangle c_j^n(t)\,, \tag{5}$$

Fig. 1. Staples used in the extended spatial smearing.

where $\langle W_{ij} \rangle = \langle \mathcal{O}_i(t) \mathcal{O}_j^\dagger(0) \rangle$ is the correlation between the meson annihilation and creation operators at time t and 0 in the smeared states i and j, respectively.

3.2. Results and conclusions

The results for the Lagrangian density in the quark–antiquark mediator plane are shown on the left side of Fig. 2. As can be seen, the tube flux becomes wider as the quark–antiquark distance is increased. To estimate the width of the flux tube we define the value $w_{1/e}$ by $\langle \mathcal{L} \rangle(w_{1/e}) = \frac{1}{e} \langle \mathcal{L} \rangle(0)$. The results for this are shown on the right side of Fig. 2.

It was predicted [2, 3] that the squared width w^2 of this flux tube diverges logarithmically as $R \to \infty$, that is $w^2 \sim w_0^2 \log \frac{R}{R_0}$, where w^2. This behavior is called "roughening". So, we can say that the flux tube roughening has been observed from $R \sim 0.4$ fm to $R \sim 1.2$ fm. However, we have not been able yet to confirm the that the behavior is logarithmic.
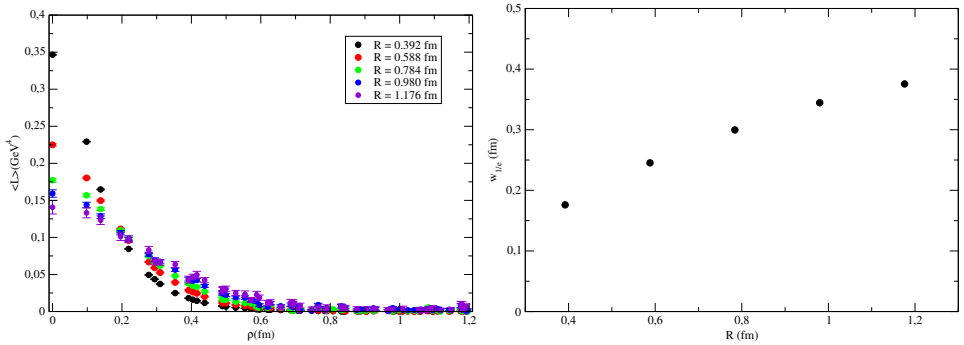

Fig. 2. Left: Lagrangian density in the mediator plane between the quark and the antiquark. Right: Width of the flux tube $w_{1/e}$ as a function of R.

4. $QQ\bar{Q}\bar{Q}$ system

Now, we consider a system of two quarks $Q_1 Q_2$ and two antiquarks $\overline{Q}_3 \overline{Q}_4$. The study of this kind of systems is important for the understanding of meson–meson scattering processes and the possible formation of tetraquarks, particles made of two valence quarks and two valence antiquarks.

In this system, we have two linearly independent color singlets. Those can be, for instance, the two meson states: $|I\rangle = \frac{1}{3}|Q_i Q_j \overline{Q}_i \overline{Q}_j\rangle$ and $|II\rangle = \frac{1}{3}|Q_i Q_j \overline{Q}_j \overline{Q}_i\rangle$, or the anti-symmetric and symmetric color states: $|A\rangle = \frac{\sqrt{3}}{2}(|I\rangle - |II\rangle)$ and $|S\rangle = \sqrt{\frac{3}{8}}(|I\rangle + |II\rangle)$. In accordance with lattice results [4, 5], the ground state could be either $|I\rangle$, $|II\rangle$ or $|A\rangle$, with the static potential being given by the flip–flop potential $V_{\text{FF}} = \min(V_I, V_{II}, V_T)$, where V_I and V_{II} are the two possible two-meson potentials, given by the sum of the intra-meson potentials, and V_T is the tetraquark potential, which confines all the particles, with the confining part being proportional to the minimal length of a fundamental string linking the four particles.

4.1. Geometries

We use the two geometries shown in Fig. 3. In both, the four particles form a rectangle, however in one of them — the parallel — similar particles are on the same side of the rectangle while on the other they are on opposite corners — the anti-parallel. With the first one, we can study the tetraquark to mesons transition, while with the second we can see the transition between the two meson states.
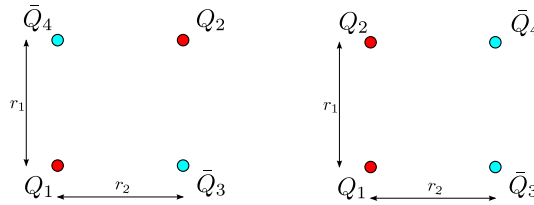

Fig. 3. Left: Anti-parallel geometry. Right: Parallel geometry.

In this work, we use 1121 Quenched $24^3 \times 48$ lattice configurations with $\beta = 6.2$. APE Smearing was applied to the spatial links, while Hyper-cubic blocking [6] was applied to the temporal links.

4.2. Variational method

To obtain not only the ground state but also the first excited state, we use a variational basis similar to Eq. (5) but using two different kind of

operators. This way, the Wilson loop which appears on Eqs. (1) and (2) is $W_n = c_n^i W_{ij} c_n^j$. The two operator basis will be formed by the $|I\rangle$ and $|II\rangle$ annihilation operators in the anti-parallel geometry and in the parallel geometry, by the $|I\rangle$ and $|A\rangle$ [4, 5] annihilation operators. This gives the matrix elements in Fig. 4.
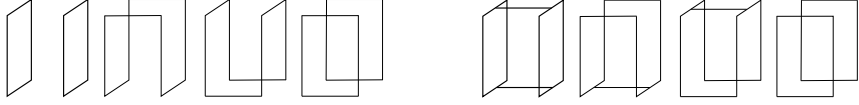

Fig. 4. Left: Loops used to study the antiparallel geometry. Right: Loops used to study the parallel geometry.

4.3. Results

The results for the Lagrangian density $\mathcal{L}$ in the ground state and the first excited state are given in Figs. 5 and 6. For the ground state the system collapses in a two meson state, when $r_2 \gg r_1$, as expected. Looking at the Wilson loop composition we also conclude that when $r_1 = r_2$ the ground state is color symmetric. The excited state is not so readily explainable. The results for $\mathcal{L}$ in the parallel geometry can be seen in Figs. 7 and 8. The results are the expected ones for the ground state, with the system passing from a two meson state to a tetraquark state as we increase r_2. We discuss the first excited state in the conclusion.
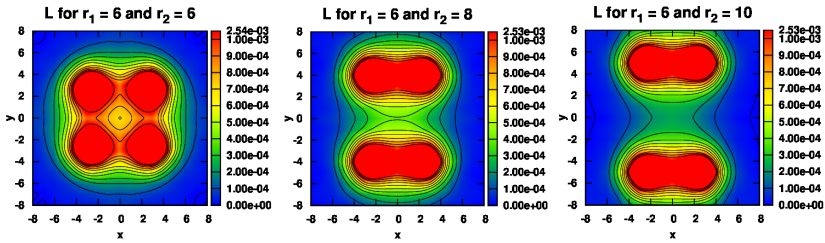

Fig. 5. Lagrangian density for the ground state of the antiparallel geometry.
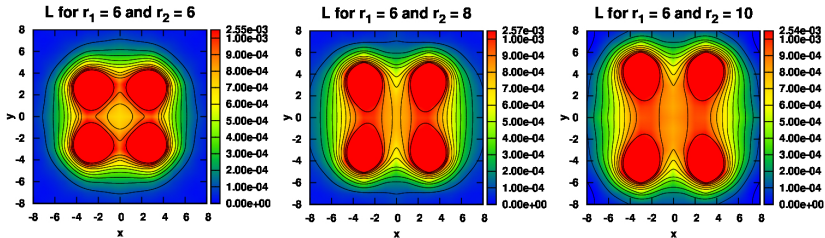

Fig. 6. Lagrangian density for the first excited state of the antiparallel geometry.
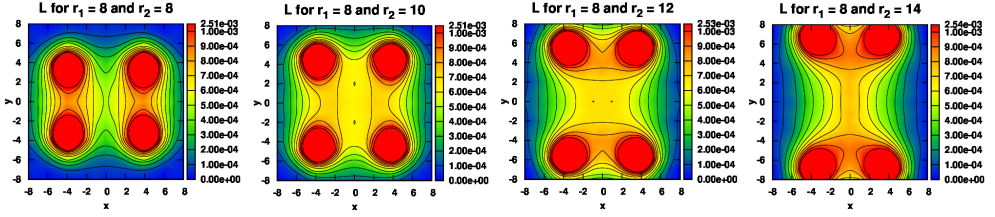
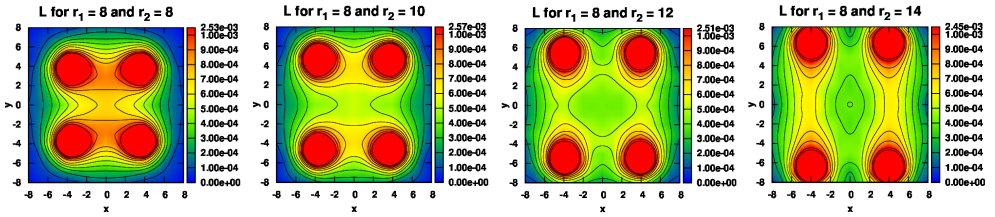Fig. 7. Lagrangian density for the ground state of the parallel geometry.

Fig. 8. Lagrangian density for the first excited state of the parallel geometry.

4.4. Discussion and conclusion

The results for the ground state are consistent with the flip–flop ground state potential with the color fields dispositions being consistent with $|I\rangle$, $|II\rangle$ or $|A\rangle$ where expected.

We can explain the excited states if we consider that the vibrational and rotational flux tube excitations effects are negligible. Therefore, the first excited state is orthogonal to the ground state. In that case, if we compute the Casimir factors for this orthogonal states, as in [7], that they predict the correct behavior of the fields, with a repulsion between particles, where we expect it.

REFERENCES

[1] G. Parisi, R. Petronzio, F. Rapuano, *Phys. Lett.* **B128**, 418 (1983).

[2] F. Gliozzi, M. Pepe, U.-J. Wiese, *Phys. Lett.* **104**, 232001 (2010).

[3] M. Luscher, G. Munster, P. Weisz, *Nucl. Phys.* **B180**, 1 (1981).

[4] C. Alexandrou, G. Koutsou, *Phys. Rev.* **D71**, 014504 (2005).

[5] F. Okiharu, H. Suganuma, T.T. Takahashi, *Phys. Rev.* **D72**, 014505 (2005).

[6] A. Hasenfratz, F. Knechtli, *Phys. Rev.* **D64**, 034504 (2001).

[7] M. Cardoso, N. Cardoso, P. Bicudo, *Phys. Rev.* **D86**, 014503 (2012).